Perturbative Approach for Fast and Accurate Evaluation of Quasi Axially-Symmetric Cavity Resonance Frequency in Drift Tube Linacs

**Giorgio S. Mauro[1, 2, *], Santi C. Pavone[1, 3], Giuseppe Torrisi[1],
Antonio Palmieri[4], Luigi Celona[1], Santo Gammino[1], and Gino Sorbello[1, 3]**

Abstract—In this paper, we present an analytical method, employable with commercial full-wave electromagnetic CADs, which allows full-wave simulations of large electromagnetic (EM) structures (i.e., in terms of wavelength), such as linear accelerator cavities (LINACs) and a very accurate estimation of their operating frequency. The proposed technique is based on the exploitation of rotational symmetry through the definition of equivalent axially-symmetric volumes which replace the non axially-symmetric ones inside the structure being analyzed. After a theoretical study, we show the successful application of the method in the real case study of a Drift Tube Linac (DTL) cell.

1. INTRODUCTION

Large EM problems in terms of operating wavelength, which often occur when dealing with the design of linear particle accelerators [1], or characterized by very small geometrical details [2, 3], result in rapidly growing mesh size and memory demand, hence simulation times may discourage or make prohibitory any automated optimization procedure. Undoubtedly, the simplest idea to reduce the required computational effort consists in making a coarse mesh to discretize EM models, in order to find an approximate solution that, at least for very regular and highly symmetric shapes or for conventional applications, can be considered satisfactory. However, such a solution cannot be applied to the case of accelerating stages of charged particles, since relative errors of a few thousands of percent in the estimation of the cavity lowest characteristic frequency result in an incorrect cavity tuning and thus in an inefficient particle acceleration. In a typical DTL cavity such as the ESS DTL, for which the quality factor Q is usually about 4×10^4 [4], a frequency error well below 0.2% is required, which corresponds to the absolute frequency of $\approx 0.7\,\text{MHz}$ for the nominal operating frequency $f_0 = 351.20\,\text{MHz}$, a typical value adopted in standard LINAC DTL cavities [5]. For this reason, any geometric detail that would produce a larger frequency detuning needs to be correctly included into the model.

To overcome such issues, analytical and numerical considerations can be made *a priori* before simulating the entire model by a brute-force approach, to efficiently control the size of the problem to be faced [6]. To this aim, the techniques usually adopted to reduce computational burden can be grouped into two families: 1) *exact* methods able to scale-down problem size, such as domain decomposition [7, 8] and reduced models that exploit geometrical symmetries [9–11] and 2) *approximate* methods based on the elimination of small geometric details that break model symmetries. Exact methods lead to a substantial reduction of the computational cost, so that reduced models are widely adopted in several practical applications. Instead, the use of approximate methods provides only qualitative results and

[1] Istituto Nazionale di Fisica Nucleare (INFN) - Laboratori Nazionali del Sud, Via S. Sofia 62, Catania 95123, Italy. [2] Dipartimento di Ingegneria dell'Informazione, delle Infrastrutture e dell'Energia Sostenibile, Università degli Studi Mediterranea di Reggio Calabria Salita Melissari, Reggio, Calabria 89124, Italy. [3] Dipartimento di Ingegneria Elettrica, Elettronica e Informatica, Università degli Studi di Catania, Viale Andrea Doria 6, Catania 95125, Italy. [4] Istituto Nazionale di Fisica Nucleare (INFN) - Laboratori Nazionali di Legnaro, Viale dell'Università 2, Legnaro 35020, Italy.

is limited to ideal scenarios, since they rely on a simplified geometric description of the problem. A more appropriate approach is based on the replacement of some geometric details with properly chosen equivalent volumes, with a more convenient geometry in terms of employed computational resources [12].

In this work, we describe a quantitative approach to deal with large quasi axially-symmetric EM problems: firstly, suitable approximations are made to simplify the cavity model without considering unnecessary geometric details, thus reducing problem size. Moreover, by using a general result of perturbation theory [13, §6.7, pag. 306], a non axially-symmetric problem is transformed in an equivalent axially-symmetric one, in which suitable fictitious equivalent volumes are introduced to predict and correct any deviation from the accelerating cavity operating frequency. Such a hybrid method is able to dramatically reduce the computational effort and to ensure a priori the required accuracy for the design of accelerating stages of linear accelerators.

The paper is divided as follows. In Section 2, the problem formulation is presented. In Section 3, the proposed method is tested numerically, and finally, in Section 4 conclusions are drawn.

2. PROBLEM FORMULATION

Exact methods that exploit mirror symmetries, translational invariance, periodicity, or even roto-translational symmetries [9–11] can be applied only in special cases. Often the object symmetry is broken, thus requiring the full geometry to be simulated: this is the case of a DTL cavity, where the internal drift tubes are connected to the tank outer wall through metallic cylinders called *stems*, as shown in Fig. 1.

Figure 1. Internal view of a DTL cold model for RF tests. The drift tubes (central elements) are connected to the tank outer wall through physical metallic supports called stems.

2.1. DTL Operation Principles

To qualitatively recall the operation principles of a DTL, we consider a rotationally-invariant circular cylindrical cavity (i.e., the so-called "pill-box" cavity) of radius a and length l, operating in the TM^z_{npq} cavity mode, labeled as usual by the integer numbers (n, p, q). For simplicity, in the following a standard cylindrical reference frame (ρ, ϕ, z) will be assumed, in which ρ, ϕ, and z denote the radial, azimuthal and axial field components, respectively. The electric field $\underline{\mathbf{E}}(\rho, \phi, z) = E_\rho \hat{\boldsymbol{\rho}} + E_\phi \hat{\boldsymbol{\phi}} + E_z \hat{\boldsymbol{z}}$, being $\hat{\boldsymbol{\rho}} = \cos\phi \hat{\mathbf{x}} + \sin\phi \hat{\mathbf{y}}$ and $\hat{\boldsymbol{\phi}} = -\sin\phi \hat{\mathbf{x}} + \cos\phi \hat{\mathbf{y}}$, can be expressed as

$$
\begin{aligned}
E_\rho(\rho, \phi, z) &\propto J_n'\left(\frac{x_{np}}{a}\rho\right) \cos\left[n(\phi - \phi_0)\right] \sin\left(\frac{q\pi}{l}z\right), \\
E_\phi(\rho, \phi, z) &\propto J_n\left(\frac{x_{np}}{a}\rho\right) \sin\left[n(\phi - \phi_0)\right] \sin\left(\frac{q\pi}{l}z\right), \\
E_z(\rho, \phi, z) &\propto J_n\left(\frac{x_{np}}{a}\rho\right) \cos\left[n(\phi - \phi_0)\right] \cos\left(\frac{q\pi}{l}z\right),
\end{aligned}
\tag{1}
$$

in which for simplicity field proportionality constants have been omitted, together with the usual time-harmonic convention $e^{+j\omega_0 t}$, where $\omega_0 = 2\pi f_0$ and f_0 the frequency. Moreover, $J_n(\cdot)$ is the n-th order Bessel function, and x_{np} is referred to the position of the p-th zeros of J_n. To accelerate charged particles along the axial z-direction only, the electric field inside the cavity is required to be oriented along the z-direction. Moreover, it does not have to exhibit azimuthal field dependence ($n = 0$) to avoid the generation of an undesired transverse kick on charged particles. All these requirements are met by exciting the TM^z_{010} cavity mode, so that $\underline{\mathbf{E}} = E_z(\rho)\hat{\mathbf{z}}$, in which

$$E_z(\rho) \propto J_0\left(\frac{x_{01}}{a}\rho\right). \tag{2}$$

The z-directed accelerating electric field is maximum on the cavity axis, which is the path of charged particles. However, to obtain net acceleration the cavity has to be modified by introducing the so called drift tubes, which are placed along the path of charged particles in the positions in which the electric field is reversed and would produce a deceleration [4]. To obtain a net energy gain, drift tubes are placed along the cavity divided in cells of increasing lengths $\beta\lambda_0 = (v/c)\lambda_0$, with $\lambda_0 = c/f_0$ being the operating wavelength and β the particle relativistic velocity, which increases as it moves along the cavity axis. In Fig. 2, the detail of the DTL cavity is shown.
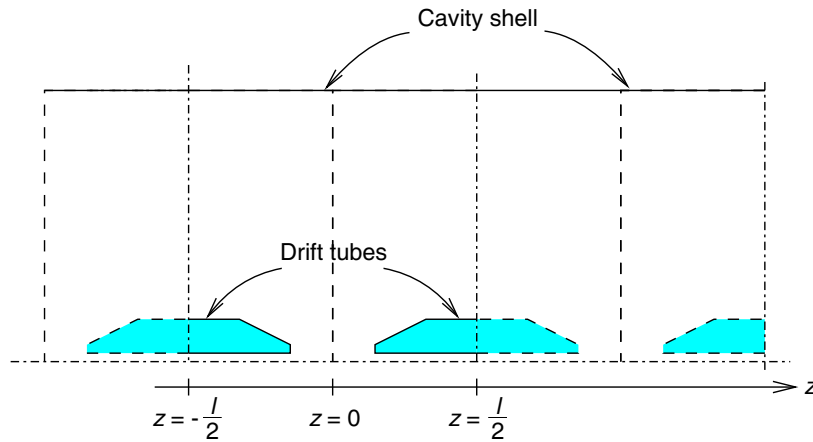

Figure 2. The DTL can be considered as a chain of accelerating cells, in which the separation between adjacent cells has been removed. The so-called drift tubes shield particles when the electric field decelerates them and concentrate the field in the gap between adjacent cells (in the figure, at $z = 0$).

Drift tubes modify the EM mode along the charged particle path without breaking the circular symmetry. The presence of drift tubes perturbs the z-uniform field distribution in Eq. (2), by introducing a new field distribution $E_z(\rho, z)$, which depends on both ρ and z, but again it does not depend on ϕ (see Fig. 3). Thus, the EM problem is azimuthally-invariant and can be solved as a 2D problem [14].
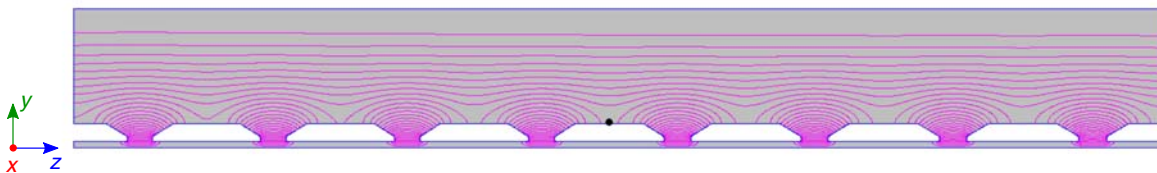

Figure 3. Multi-cell view of a DTL cavity, in which electric field lines are highlighted.

In Fig. 4(a), a perfectly rotationally-symmetric DTL half-cell, simulated with the software Superfish [15, 16], is shown. As it is apparent, the field depends on ρ and z coordinates but not on ϕ: the line of force of the electric field, $\underline{\mathbf{E}} = E_\rho\hat{\boldsymbol{\rho}} + E_z\hat{\mathbf{z}}$, is shown oi the same Fig. 4(a), while the accelerating electric field E_z along the cavity axis is shown in Fig. 4(b).
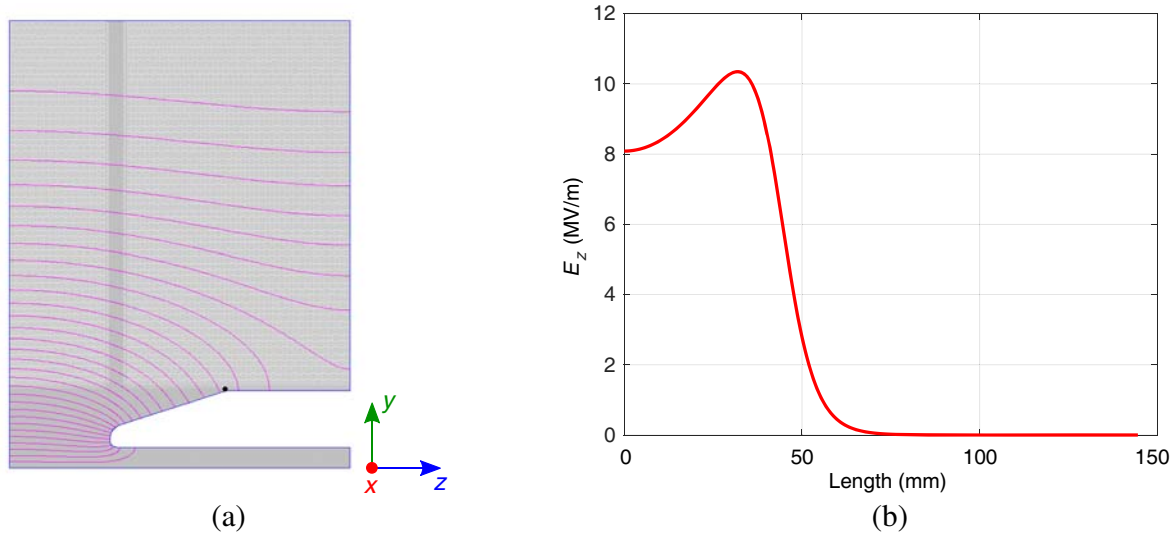
Figure 4. (a) Electric field lines of force in the Superfish DTL half-cell representation (due to the z reflection symmetry only half is actually simulated). Thanks to the rotational symmetry, a 2D problem is solved and accordingly an extremely fine mesh can be used. (b) Axial electric field, $|E_z(\rho = 0, z)|$, versus z.

However, as pointed before, in a real DTL cavity drift tubes must have physical *supports* called *stems*. The *stems* break the circular symmetry.

2.2. Real DTL Cell

The typical DTL cell geometry is shown in Fig. 5; it is apparent that a reduced model employing rotational symmetry cannot be applied, since it is broken by the presence of the stem. Only if we neglect the presence of stem, both the geometry and the EM field are perfectly rotationally-symmetric.
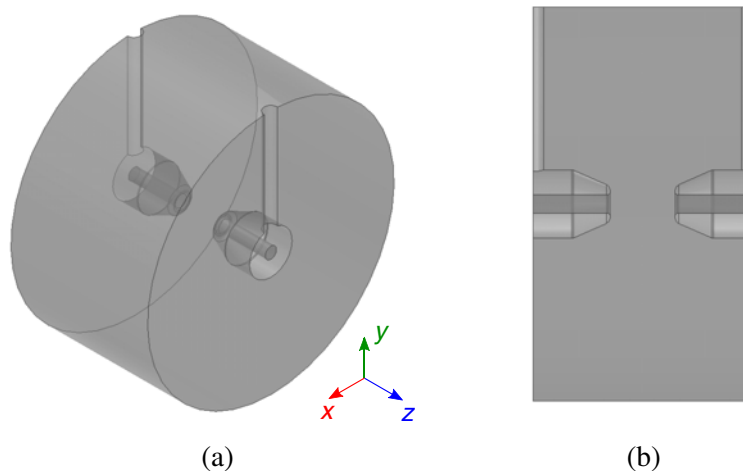

Figure 5. (a) 3D and (b) side view of a DTL cell model. The presence of stem breaks the rotational symmetry.

As a first approximation, we may leave out the stem and get through the approximate model shown in Fig. 6(a). Such a structure can be conveniently simulated either considering an angular slice like the one shown in Fig. 6(b) (i.e., a quasi-2D model [11]) or considering an exact 2D model (see Fig. 4(a)) that
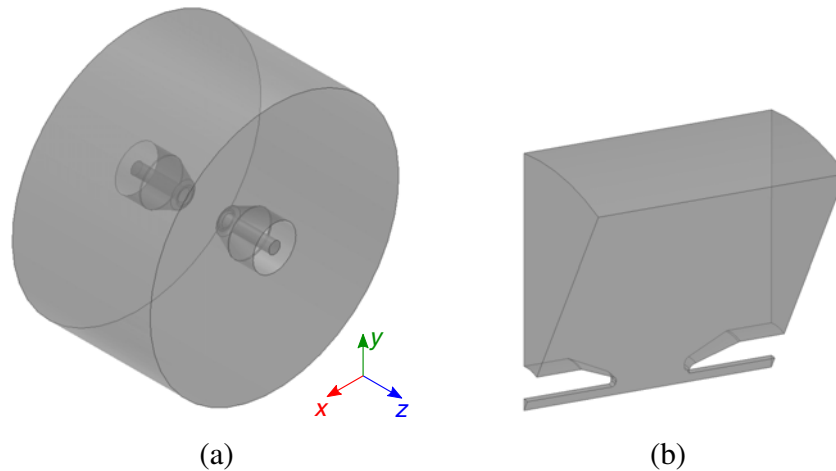
Figure 6. 3D representation of a DTL cell: (a) full structure without stem and (b) cell slice that can be conveniently simulated forcing periodic boundary condition on the two radial faces (cross sections).

considers an analytical 2π rotation (due to ϕ-invariance) in the differential equation to be solved [14]. This approximate and oversimplified lower-dimensionality approach provides only qualitative results. Nevertheless, it is often adopted for reasoning in all the study cases in which precise quantitative results are not required.

However, in the case at hand, this approximate model can be affected by a large frequency error, providing only qualitative information that cannot be used for DTL fine tuning. Indeed, although stems are located in a region of the cavity in which they introduce almost no perturbation on the accelerating axial electric field, their presence affects the EM field in the volume in which they are inserted. Consequently, the presence of stems results in a "large" shift of cavity resonant frequency, thus they cannot be safely neglected and removed from the cavity model.

2.3. Numerical Error Compensation

As outlined previously, the stem breaks the rotational symmetry of the DTL cell. As a first approximation, one could try to remove this component in the simulated model, in such a way to restore the lost symmetry. However, a noticeable frequency error arises, since the cavity resonant frequency increases if a volume ΔV is subtracted (by inserting a metal object) in a region in which strong magnetic and weak electric fields are present. This is the case of stems, which are located in such regions. Vice versa by neglecting them, a volume is added to the cavity, and the simulated cavity resonance frequency decreases.

To overcome such an issue, here we propose a numerical method able to take into account the presence of symmetry-breaking stems. According to basic EM theory, in a resonant cavity stored magnetic and electric energies are balanced. When the cavity is perturbed (in our case the perturbation is due to virtual stem presence/removal), the "perturbation" produces a displacement of electric and magnetic energies and in turn a frequency shift to restore it [4]. Such a frequency error can be predicted and corrected. Let us consider an ideal unperturbed cavity (#1) with no stems, resonance frequency f_1, and volume V_1, and a perturbed cavity (#2) with resonance frequency $f_2 = f_1 + \Delta f$ and volume $V_2 = V_1 - \Delta V$, in which ΔV accounts for the volume subtracted from the cavity by the presence of stems. For simplicity, in the unperturbed cavity #1 the EM field is labeled by $\{\underline{\mathbf{E}}_1, \underline{\mathbf{H}}_1\}$, whereas in the perturbed cavity #2 the EM field is labeled by $\{\underline{\mathbf{E}}_2, \underline{\mathbf{H}}_2\}$. The stem is placed in a region of the cavity in which it does not significantly alter the EM field distribution, hence we can safely assume $\{\underline{\mathbf{E}}_2, \underline{\mathbf{H}}_2\} \approx \{\underline{\mathbf{E}}_1, \underline{\mathbf{H}}_1\} = \{\underline{\mathbf{E}}, \underline{\mathbf{H}}\}$.

According to [13, Eq. (6.107)], the approximate relative variation of the resonant frequency can be

written as

$$\frac{\Delta f}{f_1} = \frac{\Delta \omega}{\omega_1} \approx \frac{\iiint_{\Delta V} (\mu_0 |\underline{\mathbf{H}}|^2 - \epsilon_0 |\underline{\mathbf{E}}|^2) \mathrm{d}V}{\iiint_{V} (\mu_0 |\underline{\mathbf{H}}|^2 + \epsilon_0 |\underline{\mathbf{E}}|^2) \mathrm{d}V} = \frac{\Delta U_m - \Delta U_e}{U}, \tag{3}$$

where

$$\Delta U_m = \frac{1}{4} \iiint_{\Delta V} \mu_0 |\underline{\mathbf{H}}|^2 \mathrm{d}V, \tag{4}$$

and

$$\Delta U_e = \frac{1}{4} \iiint_{\Delta V} \epsilon_0 |\underline{\mathbf{E}}|^2 \mathrm{d}V \tag{5}$$

are the time-averaged stored magnetic and electric energies removed by the perturbing volume/object ΔV, respectively, whereas

$$U = \frac{1}{4} \iiint_{V} (\mu_0 |\underline{\mathbf{H}}|^2 + \epsilon_0 |\underline{\mathbf{E}}|^2) \mathrm{d}V \tag{6}$$

is the total stored energy inside the cavity with volume $V = V_1$. We will use Eq. (3) to first predict and then correct the frequency error introduced by the presence of the stem or by any geometric approximations. The prediction is based on the application of Eq. (3) with $\Delta V = V_{\text{real-stem}}$. The correction is based on a model representing the DTL cell with a "virtual stem volume" $\Delta V = V_{\text{virtual-stem}}$, which correctly accounts for the frequency shift introduced by the real stem, without breaking the rotational symmetry, thus allowing 2D or quasi-2D simulation.

The virtual stem volume can be calculated by relating the magnetic field in the region that the "virtual stem" is placed and the average magnetic field along the real stem, since both real and virtual stems lay in a region of low electric energy density, which is $\frac{1}{2}\epsilon_0 |\underline{\mathbf{E}}|^2$. Hence, we can consider only the displacement in magnetic field energy density, $\frac{1}{2}\mu_0 |\underline{\mathbf{H}}|^2$. To compensate the frequency shift we require that the total "removed" magnetic energy, ΔU_m, is left unchanged in both scenarios. We enforce the same ΔU_m when we consider the real stem ($\Delta V = V_{\text{real stem}}$), and then a virtual rotationally-symmetric stem ($\Delta V = V_{\text{virtual stem}}$), so that

$$\iiint_{V_{\text{real stem}}} \mu_0 |\underline{\mathbf{H}}|^2 \mathrm{d}V = \iiint_{V_{\text{virtual stem}}} \mu_0 |\underline{\mathbf{H}}|^2 \mathrm{d}V \tag{7}$$

$$S \underbrace{\int_{L_{\text{stem}}} |\underline{\mathbf{H}}|^2 \mathrm{d}L}_{=H_{\text{L-avg}}^2 L_{\text{stem}}} = \underbrace{\iiint_{V_{\text{virtual stem}}} |\underline{\mathbf{H}}|^2 \mathrm{d}V}_{=H_{\text{V-avg}}^2 V_{\text{virtual stem}}} \tag{8}$$

where $S = \pi r_{\text{stem}}^2$ is the real stem cross-section. It should be noticed that since $r_{\text{stem}} \ll \lambda_0$, the volume integral in Eq. (7) can be reduced to a line integral; in Eq. (8) the line-averaged (volume-averaged) magnetic field $H_{\text{L-avg}}$ ($H_{\text{V-avg}}$) is also implicitly defined, so that Eq. (8) can be written as

$$\frac{1}{2} S L_{\text{stem}} H_{\text{L-avg}}^2 \approx V_{\text{virtual stem}} H_{\text{V-avg}}^2, \tag{9}$$

Equation (9) can be used to derive the required $V_{\text{virtual stem}}$ from the real stem geometric parameters, S and L_{stem} (stem length), once knowing the ratio $(H_{\text{L-avg}}/H_{\text{V-avg}})^2$. The factor $1/2$ in Eq. (9) has been inserted to take into account that only half-cell (half stem) is considered in the calculation.

3. NUMERICAL VALIDATION

Let us consider the 3D scenario in Fig. 5 and the 2D cross section in Fig. 7, in which the relevant geometrical parameters are reported in Table 1. By assuming a total stored energy inside the cavity equal to $U = 0.81\,\text{J}$, the average magnetic field has been evaluated along the stem height, so that
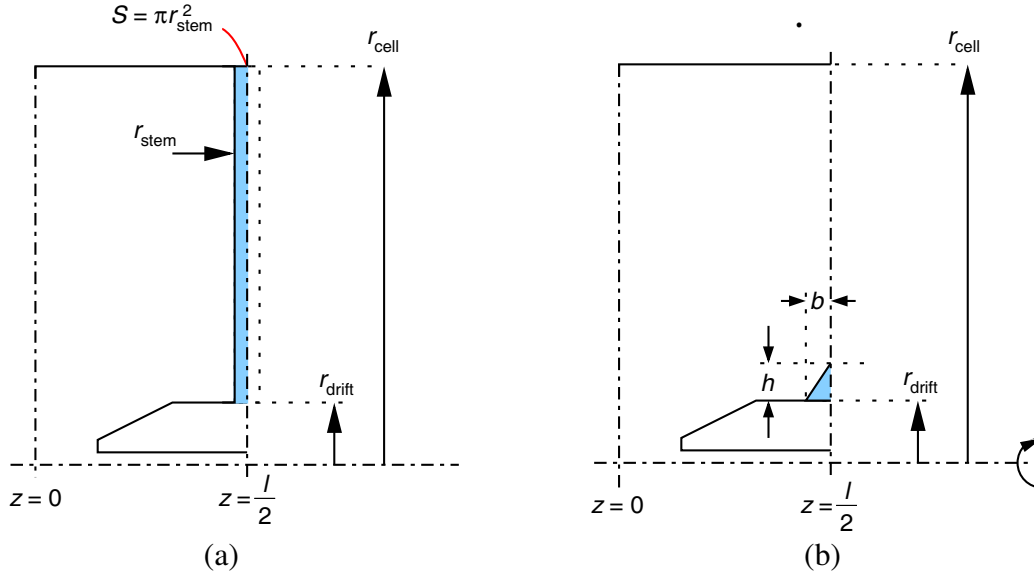
Figure 7. Half DTL cell. Blue highlighted areas are (a) real and (b) virtual stem.

Table 1. Relevant geometrical parameters.

Parameter	Value (m)	Value (λ_0)	Description
r_{cell}	0.2605	0.305	cell radius
l	0.2890	0.338	cell length
$L_{\text{stem}} = r_{\text{cell}} - r_{\text{drift}}$	0.2155	0.252	stem length
r_{stem}	0.014	0.016	stem radius

$H_{\text{L-avg}} = \left(\frac{1}{L_{\text{stem}}} \int_{r_{\text{drift}}}^{r_{\text{cell}}} |\underline{\mathbf{H}}(\rho, z = \frac{l}{2})|^2 dr \right)^{\frac{1}{2}} \simeq 5758 \, \text{A/m}$. If the stem volume is neglected, it would lead to a relative frequency error of $\frac{\Delta f}{f_0} \approx \frac{\Delta U_m}{U} \approx \frac{\frac{\mu_0}{4} S L_{\text{stem}} H_{\text{L-avg}}^2}{U} \approx 0.3\%$, where $f_0 = 351.20 \, \text{MHz}$.

The rotationally-symmetric volume that has to replace the real stem can be arbitrary shaped, but it is useful to choose a canonical one to make calculations simpler. Hence, let us consider a triangular surface and the volume obtained by rotating it around the cell symmetry axis, so that $V_{\text{virtual stem}} = 2\pi r_{\text{drift}} \left(\frac{1}{2} hb \right)$, in which r_{drift} is the external radius of the drift tube, and h, b are the triangle height and base, as shown in Fig. 7(b).

By considering that the magnetic field in a DTL cell is dominantly concentrated in the neighborhood on its outer wall, i.e., close to $(\rho, z) = (r_{\text{drift}}, l/2)$ (Fig. 7(b)), the magnetic energy associated with the virtual stem can be approximated as ΔU_m in Eq. (4), with $\Delta U_m \propto H_{\text{V-avg}}^2 V_{\text{virtual stem}} = H_{\text{V-avg}}^2 \pi r_{\text{drift}} hb$. The magnetic field is calculated as $H_{\text{V-avg}} \approx |\underline{\mathbf{H}}(\rho = r_{\text{drift}}, z = l/2)| \approx 10264 \, \text{A/m}$, in which the reference value of $U = 0.81 \, \text{J}$ for the total stored energy inside the cavity is assumed. From Eq. (9), the virtual stem volume is

$$V_{\text{virtual stem}} \approx \frac{H_{\text{L-avg}}^2}{H_{\text{V-avg}}^2} \frac{1}{2} S L_{\text{stem}} = \frac{H_{\text{L-avg}}^2}{H_{\text{V-avg}}^2} \frac{1}{2} \pi r_{\text{stem}}^2 L_{\text{stem}}, \tag{10}$$

where r_{stem} is the stem radius. By substituting appropriate numerical values, one finds $V_{\text{virtual stem}} \simeq 20879 \, \text{mm}^3$. By arbitrarily fixing the triangle height to $h = 25 \, \text{mm}$, the triangle base b can be easily evaluated as $b = \frac{V_{\text{virtual stem}}}{\pi r_{\text{drift}} h}$. The determined triangle base is $b \simeq 6 \, \text{mm}$.

The cell has been simulated in CST by considering the calculated volume (quasi-2D model) as shown in Fig. 8, i.e., a cell angular sector of 90°. An operating frequency of $f_1 \simeq 350.95 \, \text{MHz}$ has
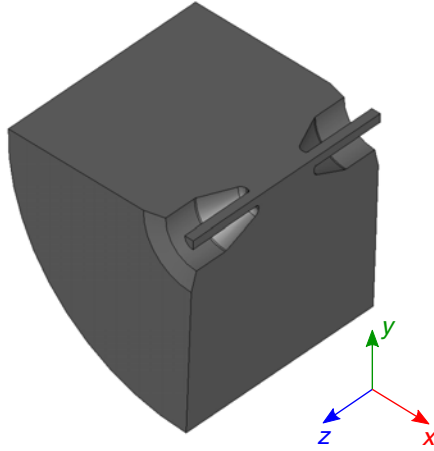
Figure 8. Application of the equivalent volume method to a DTL cell using CST commercial simulator, where only an angular sector of 90° has been simulated. A normal deviation angle [17] of $\alpha = 5°$ is also used to ensure accurate results [6].

been found, which is in good agreement with that found by considering a full 3D simulation of the cell comprising the real stem ($f_0 = 351.20\,\text{MHz}$).

The quasi-2D method can be easily extended at a multicell cavity with minor calculation effort. For validation, a DTL tube composed of six cells of the ESS DTL tank 4 with different lengths has been simulated. For each cell, the numerical method has been applied, and appropriate rotationally symmetric triangular volumes have been introduced. The approximation error does not accumulate for a multi-cell cavity as compared to a single cell cavity, provided that the equivalent volumes are correctly calculated for each cell. For the multi-cell DTL of six cells, the numerical error results $\frac{\Delta f}{f_0} \simeq 0.06\%$, almost equal to the single-cell one.

It is worth mentioning that the applicability of the proposed method requires the basic underlying hypothesis of *perturbation method* to be satisfied, i.e., it is required that the actual field of the modified cavity does not differ significantly from the reference one.

In the case of a DLT cell we are interested only in the accelerating on axis electric field, which is large only between the two drift tube halves. Moreover, the metallic volumes are inserted in a region with a predominance of magnetic field: so the on-axis electric field is not much affected by the insertion of the triangular equivalent volume or by the insertion of the real stem. However, this could not be the case if one considers different geometries.

For completeness, in Table 2 we report the simulation time required for 2D, quasi-2D (angular sector of 90°), and full 3D simulations of the DTL cell. For the 2D simulation, Superfish has been adopted, and it can be noticed that the simulation time is extremely fast with respect to the full 3D simulation (a factor of 120 for a single cell). It can also be seen that the quasi-2D simulation performed with the presented method employs about 1/3 of the time required for a full 3D simulation of the same cell comprising the real stem volume.

It should be emphasized that the time required for the full 3D simulation (approx. six minutes) refers to a single DTL cell. Actually, a complete DTL is composed of roughly 30 coupled cells (such as the case of the tanks 2 to 5 of the ESS DTL), resulting in a dramatic increase of computational effort for

Table 2. Comparison between 3D, quasi-2D and 2D simulation times and mesh elements used.

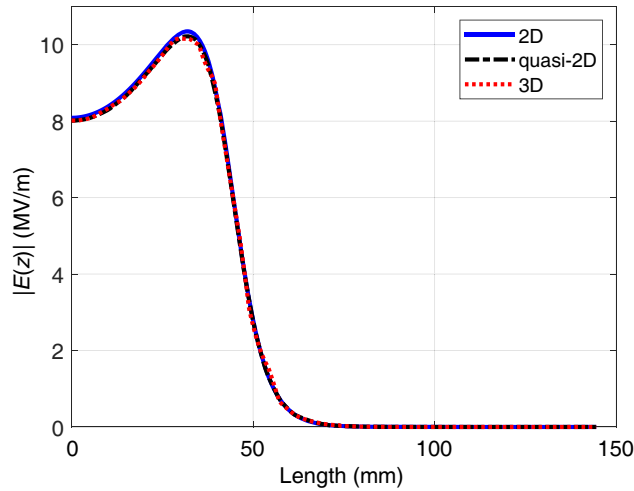|	3D	quasi-2D	2D
Mesh elements	188190	88363	87360
Simulation time	6 m	2 m: 30 s	3 s

Figure 9. Electric field along the longitudinal z direction for half DTL cell obtained with 3D, quasi-2D and 2D simulations. The 2D simulation does not take into account stem presence; however, apart from a frequency shift, this has no impact on the on-axis electric field.

simulating the full 3D structure with real stem volumes. For instance, using Ansys HFSS [17], the full 3D simulation of the DTL tank 4 of the ESS project results in a mesh about 6.3 million of elements and requires a simulation time about 6 h, by using 192 GB of RAM and a multi-core processor (14 cores). In the latter case, the full structure simulation results are strongly aided by using the quasi-2D method here proposed, in terms of both time and saved computational memory.

In Fig. 9, the on-axis accelerating electric field inside the DTL cell, E_z, is compared quantitatively among the 2D, quasi-2D, and 3D simulations; it can be observed that the approximation introduced has no impact on the axial field as well as on particle energy gain. By taking the electric field of the 2D simulation as the reference case (due to the extremely fine mesh used), the computed quantitative errors, intended as the maximum field value difference between the 2D simulation vs. the quasi-2D and the full 3D simulation, are respectively 1.24% and 1.86%. For our purposes, these differences are absolutely tolerable, and the three field results can be considered in excellent agreement.

4. CONCLUSIONS

In this work, an analytical relation to predict and compensate the numerical error introduced by a local geometrical approximation is proposed; the presented variational formula allows to restore rotational symmetry in large DTL resonant tanks/cavities. The method has been tested through simulations, returning good results if small non rotationally-symmetric volumes in the model are replaced by equivalent rotationally-symmetric ones. The procedure has been validated on a DTL cell model and allowed to compensate the frequency shift Δf relative to the real stem by introducing an analytically derived equivalent volume. The obtained numerical results show that it is quite accurate. The possibility to carry out much faster quasi-2D simulations, by enforcing at the same time a very fine mesh and by considering the stem presence, allowed a very fine tuning of the ESS DTL tanks without being stranded with computationally expensive 3D simulations. As an example, the application of the presented method during the numerical tuning of the ESS DTL tank 2 allowed the realization of a cold model for RF tests with measured resonant frequency of $f_0 = 351.35$ MHz.

REFERENCES

1. Aloisio, M. and P. Waller, "Analysis of helical slow-wave structures for space TWTs using 3-D electromagnetic simulators," *IEEE Trans. on Electron Devices*, Vol. 52, No. 5, 749–754, 2005.
2. Di Paola, C., K. Zhao, S. Zhang, and G. F. Pedersen, "A novel lens antenna design based on a bed of nails metasurface for new generation mobile devices," *The 14th European Conference on Antennas and Propagation European Conference on Antennas and Propagation*, IEEE, 2020.
3. Pavone, S. C., E. Martini, M. Albani, S. Maci, C. Renard, and J. Chazelas, "A novel approach to low profile scanning antenna design using reconfigurable metasurfaces," *2014 International Radar Conference*, 1–4, 2014.
4. Wangler, T. P., *RF Linear Accelerators*, Wiley-VCH, 2008.
5. https://europeanspallationsource.se/accelerator/linac, online; accessed 2 February 2020.
6. Mauro, G. S., A. Palmieri, F. Grespan, G. Torrisi, O. Leonardi, L. Celona, G. Sorbello, and A. Pisent, "Analytical method, based on slater perturbation theorem, to control frequency error when representing cylindrical structures in 3D simulators," *2019 13th European Conference on Antennas and Propagation (EuCAP)*, 1–4, IEEE, 2019.
7. Li, Y.-J. and J.-M. Jin, "A new dual-primal domain decomposition approach for finite element simulation of 3-D large-scale electromagnetic problems," *IEEE Trans. Antennas Propag.*, Vol. 55, No. 10, 2803–2810, 2007.
8. Zhang, H.-X., L. Huang, L. Zhou, Z. Zhao, Y.-T. Zheng, G. Zhu, and W.-Y. Yin, "Massively parallel simulation of antenna array using domain decomposition method and a high-performance computing scheme," *2019 IEEE International Symposium on Antennas and Propagation and USNC-URSI Radio Science Meeting*, 1251–1252, IEEE, 2019.
9. Oskooi, A. F., D. Roundy, M. Ibanescu, P. Bermel, J. D. Joannopoulos, and S. G. Johnson, "MEEP: A flexible free-software package for electromagnetic simulations by the FDTD method," *Computer Physics Communications*, Vol. 181, No. 3, 687–702, 2010.
10. Castorina, G., G. Torrisi, G. Sorbello, L. Celona, and A. Mostacci, "Conductor losses calculation in two-dimensional simulations of H-plane rectangular waveguides," *J. of Electromagnet. Wave*, Vol. 33, No. 8, 981–990, 2019.
11. Aloisio, M. and G. Sorbello, "One-third-of-pitch reduction technique for the analysis of ternary azimuthally periodic helical slow-wave structures," *IEEE Trans. Electron Devices*, Vol. 53, No. 6, 1467–1473, 2006.
12. https://uspas.fnal.gov/materials/04UW/SNS Front-End.ppt.pdf, online; accessed 2 February 2020.
13. Pozar, D., *Microwave Engineering*, 4th Edition, Wiley, 2012.
14. Chen, Y., R. Mittra, and P. Harms, "Finite-difference time-domain algorithm for solving Maxwell's equations in rotationally symmetric geometries," *IEEE Trans. Microw. Theory Techn.*, Vol. 44, No. 6, 832–839, 1996.
15. "Los Alamos National Laboratory, Superfish."
16. Halbach, K. and R. Holsinger, "SUPERFISH — A computer program for evaluation of RF cavities with cylindrical symmetry," *Particle Accelerators*, Vol. 7, 213–222, 1976.
17. ANSYS HFSS, Ansoft Corp., Pittsburgh, PA.